



# Critical role of the CD44<sup>low</sup>CD62L<sup>low</sup> CD8<sup>+</sup> T cell subset in restoring antitumor immunity in aged mice

Yuka Nakajima<sup>a</sup>, Kenji Chamoto<sup>a</sup>, Takuma Oura<sup>a</sup>, and Tasuku Honjo<sup>a,1</sup>

<sup>a</sup>Department of Immunology and Genomic Medicine, Center for Cancer Immunotherapy and Immunobiology, Kyoto University Graduate School of Medicine, Kyoto 606-8501, Japan

Contributed by Tasuku Honjo, April 29, 2021 (sent for review February 24, 2021; reviewed by Yutaka Kawakami and Hiroshi Shiku)

**CD8<sup>+</sup> T cells play a central role in antitumor immune responses that kill cancer cells directly. In aged individuals, CD8<sup>+</sup> T cell immunity is strongly suppressed, which is associated with cancer and other age-related diseases. The mechanism underlying this age-related decrease in immune function remains largely unknown. This study investigated the role of T cell function in age-related unresponsiveness to PD-1 blockade cancer therapy. We found inefficient generation of CD44<sup>low</sup>CD62L<sup>low</sup> CD8<sup>+</sup> T cell subset (P4) in draining lymph nodes of tumor-bearing aged mice. In vitro stimulation of naive CD8<sup>+</sup> T cells first generated P4 cells, followed by effector/memory T cells. The P4 cells contained a unique set of genes related to enzymes involved in one-carbon (1C) metabolism, which is critical to antigen-specific T cell activation and mitochondrial function. Consistent with this finding, 1C-metabolism-related gene expression and mitochondrial respiration were down-regulated in aged CD8<sup>+</sup> T cells compared with young CD8<sup>+</sup> T cells. In aged OVA-specific T cell receptor (TCR) transgenic mice, ZAP-70 was not activated, even after inoculation with OVA-expressing tumor cells. The attenuation of TCR signaling appeared to be due to elevated expression of CD45RB phosphatase in aged CD8<sup>+</sup> T cells. Surprisingly, strong stimulation by nonself cell injection into aged PD-1-deficient mice restored normal levels of CD45RB and ameliorated the emergence of P4 cells and 1C metabolic enzyme expression in CD8<sup>+</sup> T cells, and antitumor activity. These findings indicate that impaired induction of the P4 subset may be responsible for the age-related resistance to PD-1 blockade, which can be rescued by strong TCR stimulation.**

aging | PD-1 | immunotherapy | T cell subset | one-carbon metabolism

**A**ging affects numerous physiological functions, resulting in the onset of a variety of diseases. Cancer risk increases with age, as mutations accumulate in the genome and immune surveillance against cancer cells gradually declines (1, 2). Immunotherapy that reactivates tolerized immune function has emerged as an effective strategy for treating cancer. Among the array of cancer immune therapeutics, antibodies that block the PD-1/PD-L1 pathway have yielded highly promising results in patients with a broad spectrum of cancers (3–6). However, clinical studies have shown that many cancer patients are unresponsive to PD-1 blockade therapy (7, 8). The efficacy of such therapy is impaired in aged-mouse models, with similar attenuation to that observed in some clinical reports (9–12).

Immune senescence results from quantitative and/or qualitative changes in immune cells. One of the major quantitative changes in T cells is the decline of the T cell receptor (TCR) repertoire diversity due to thymic involution, reducing the output of naive cells into the periphery (13–15). In addition, peripheral T cells in aged individuals accumulate qualitative defects such as impaired TCR signaling, diminished differentiation capacity to effector and memory cells, and reduced cytokine production (16, 17). In fact, age-associated changes strongly affect the frequency of well-defined CD8<sup>+</sup> T cell subsets (18–20). CD44 and CD62L (L-selectin) surface markers were used to define three major subsets of CD8<sup>+</sup> T cells in mice: naive (also called P1; CD44<sup>low</sup>CD62L<sup>high</sup>), central memory (P2; CD44<sup>high</sup>CD62L<sup>high</sup>), and effector/memory (P3; CD44<sup>high</sup>CD62L<sup>low</sup>). The remaining CD44<sup>low</sup>CD62L<sup>low</sup> (P4) CD8<sup>+</sup>

T cell subset is a very minor population in naive mice and has been rarely studied. Naive T cells differentiate into effector T cells by antigenic stimulation (14, 21). Some effector cells become memory cells, which quickly give rise to effector cells in response to the same antigenic stimulation. In aged humans and animals, T cell maintenance requires self-antigen-dependent proliferation (homeostatic proliferation) because of the decline in T cell output from the thymus (22, 23). In aged individuals, this homeostatic proliferation gradually boosts naive T cell differentiation, resulting in an increased frequency of differentiated T cell subsets including effector and memory cells.

T cell proliferation and differentiation are promoted by TCR signaling cascades. The phosphorylation and dephosphorylation of TCR signaling molecules affect signaling complex formation and the propagation of TCR signals. CD45 is a transmembrane phosphatase that plays a central role in the modulation of TCR signaling by controlling the level of tyrosine phosphorylation of lymphocyte protein kinase (Lck), which serves as an activator of TCRζ-chain-associated protein (ZAP)-70, and the linker of activated T cells (LAT) (24, 25). In young naive and memory CD8<sup>+</sup> T cells, high CD45 expression inhibits TCR signal transduction through dephosphorylation of ZAP-70 and PLCγ (26). While aging is known to alter TCR signaling, the molecular mechanisms underlying these changes remain largely unclear (27, 28).

In activated and proliferating cells, one-carbon (1C) metabolism is generally up-regulated, supporting their survival and differentiation through promoting biosynthesis of purine and thymidine, amino acid homeostasis, epigenetic maintenance, and redox defense

## Significance

**Although aging is known to suppress antitumor immunity, the precise underlying mechanism remains largely unknown. Here, we found that the inefficient generation of CD44<sup>low</sup>CD62L<sup>low</sup> CD8<sup>+</sup> T cell subset (P4), pre-effector-like T cells, could explain the resistance to PD-1 blockade antitumor therapy in aged mice. Elevated expression of CD45RB in aged naive CD8<sup>+</sup> T cells appears to inhibit TCR signaling, resulting in fewer P4 cells, a subset with high expression of 1C metabolic genes. This decrease in P4 cells and antitumor activity was rescued by strong immunogenic stimulation by nonself cells. These findings provide valuable insights into the mechanism underlying age-induced suppression of antitumor immunity, which may provide a basis for the development of therapeutic strategies for elderly cancer patients.**

Author contributions: Y.N., K.C., and T.H. designed research; Y.N., K.C., and T.O. performed research; Y.N. and T.O. analyzed data; and Y.N., K.C., and T.H. wrote the paper.

Reviewers: Y.K., International University of Health and Welfare; and H.S., Mie University School of Medicine.

The authors declare no competing interest.

Published under the PNAS license.

<sup>1</sup>To whom correspondence may be addressed. Email: honjo@mfour.med.kyoto-u.ac.jp.

This article contains supporting information online at <https://www.pnas.org/lookup/suppl/doi:10.1073/pnas.2103730118/-DCSupplemental>.

Published June 4, 2021.

(29, 30). Recent reports indicate that 1C metabolism is one of the most strongly induced metabolic pathways during early CD4<sup>+</sup> or CD8<sup>+</sup> T cell activation (31, 32). After T cell activation, up-regulation of the 1C metabolic network increases the processing of serine to provide de novo nucleotide biosynthesis from one-carbon units, which is required for antigen-specific T cell proliferation, differentiation, and effector functions. The 1C metabolic pathways also contribute to energy production through the regulation of mitochondrial protein synthesis by mitochondrial tRNA methylation (33, 34). Mitochondrial function and 1C metabolism are lower in aged than in young CD4<sup>+</sup> T cells (35), suggesting a possible link between T cell aging and the inactivation of 1C metabolism.

To elucidate the mechanism underlying age-related attenuation of the antitumor effect of PD-1 blockade, we compared CD8<sup>+</sup> T cells from young and aged PD-1 knockout (KO) or wild type (WT) mice with or without tumors. Here, we show that resistance to PD-1 deficiency or blockade antitumor therapy in aged mice depends on inefficient generation of the P4 subset, which is an intermediate between the naive and effector subsets and highly expresses genes related to 1C metabolism. This inhibition in aged mice is due to TCR signal suppression through elevated expression of CD45RB and can be rescued by strong immune stimulation. These findings provide insights into the mechanisms by which age-dependent changes in CD8<sup>+</sup> T cell subsets contribute to metabolic alterations and antitumor activity.

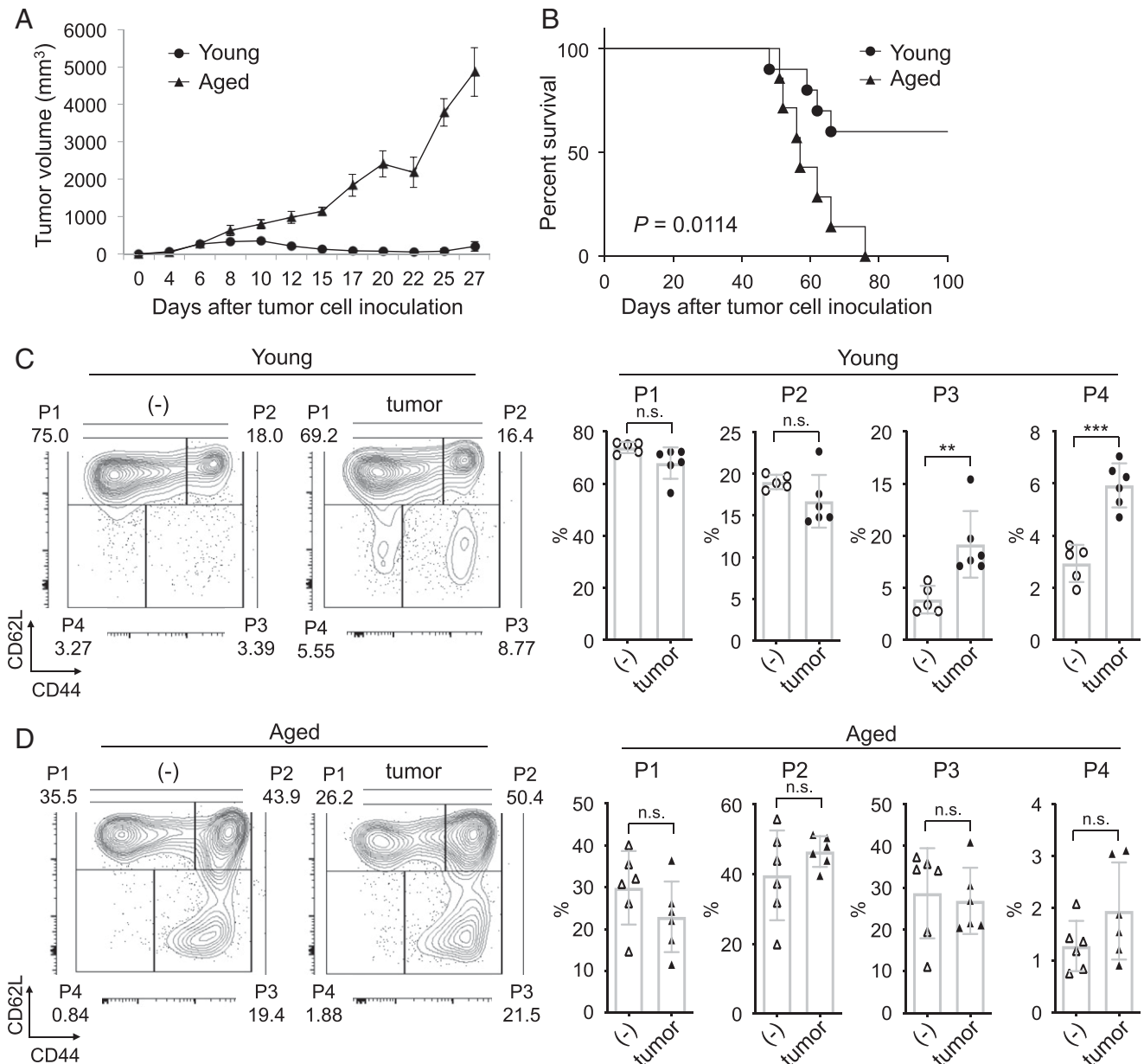


**Fig. 1.** Loss of antitumor activity and reduced P4 cell induction in aged PD-1 KO mice. (A and B) MC38 cells were i.d. inoculated into young and aged PD-1 KO mice. (A) MC38-tumor sizes in young (3–4 mo old) and aged (15 mo old) PD-1 KO mice. (B) Kaplan–Meier plot of percent survival of MC38-tumor-bearing PD-1 KO mice. (C and D) Analysis of CD8<sup>+</sup> T cell subsets in young (C) (2–3 mo old) or aged (D) (15–21 mo old) PD-1 KO mice with or without injection of MC38 cells. Stained PLN and DLN cells on day 9. Representative plots showing CD44 and CD62L expression gated on CD3<sup>+</sup>CD8<sup>+</sup> T cells and percentage of CD8<sup>+</sup> T cell subsets; CD44<sup>low</sup>/CD62L<sup>high</sup> (naive; P1), CD44<sup>high</sup>/CD62L<sup>high</sup> (central memory; P2), CD44<sup>high</sup>/CD62L<sup>low</sup> (effector/memory; P3), and CD44<sup>low</sup>/CD62L<sup>low</sup> (P4). *P* values were calculated by log-rank test or two-tailed unpaired Student's *t* test. \*\**P* < 0.01; \*\*\**P* < 0.001; n.s., not significant. Data are presented as the mean ± SEM (*n* = 8–10 for A and B; *n* = 5–6 for C and D).

**Results**

**Impaired Induction of CD44<sup>low</sup>CD62L<sup>low</sup> (P4) CD8<sup>+</sup> T Cells in Aged Mice.**

Aged PD-1 KO mice became permissive to colon carcinoma MC38 growth, while young PD-1 KO mice were strongly resistant to tumor growth (Fig. 1A and B). We also observed that aged WT mice were resistant to PD-1 blockade tumor therapy (SI Appendix, Fig. S1A and B). Comparative analysis of CD8<sup>+</sup> T cell subsets in cells of peripheral lymph nodes (PLNs) and draining lymph nodes (DLNs) from PD-1 KO mice with or without MC38 tumors showed that the percentage of the minor CD8<sup>+</sup> T cell subset P4 was substantially increased by MC38 tumor inoculation in young mice but not in aged mice (Fig. 1C and D). Changes in other CD8<sup>+</sup> T cell

subsets in response to tumor inoculation were smaller than that of the P4 subset in both young and aged PD-1 KO mice (Fig. 1C and D). Similar results were obtained in WT mice (SI Appendix, Fig. S1C and D), and in the PD-1 KO mice inoculated with different tumor, glioblastoma GL261 cells (SI Appendix, Fig. S2A–C). We next investigated the effect of tumor inoculation on each CD4<sup>+</sup> T cell subset of young and aged mice. The percentage of CD4<sup>+</sup> CD44<sup>low</sup>CD62L<sup>low</sup> (P4) subset from WT and PD-1 KO mice was not increased by MC38 tumor inoculation (SI Appendix, Fig. S3A–D), indicating that the differentiation pattern of CD8<sup>+</sup> T cells was different from the pattern of CD4<sup>+</sup> T cells. These results suggest that the P4 subset in CD8<sup>+</sup> T cells is inducible during tumor rejection and may

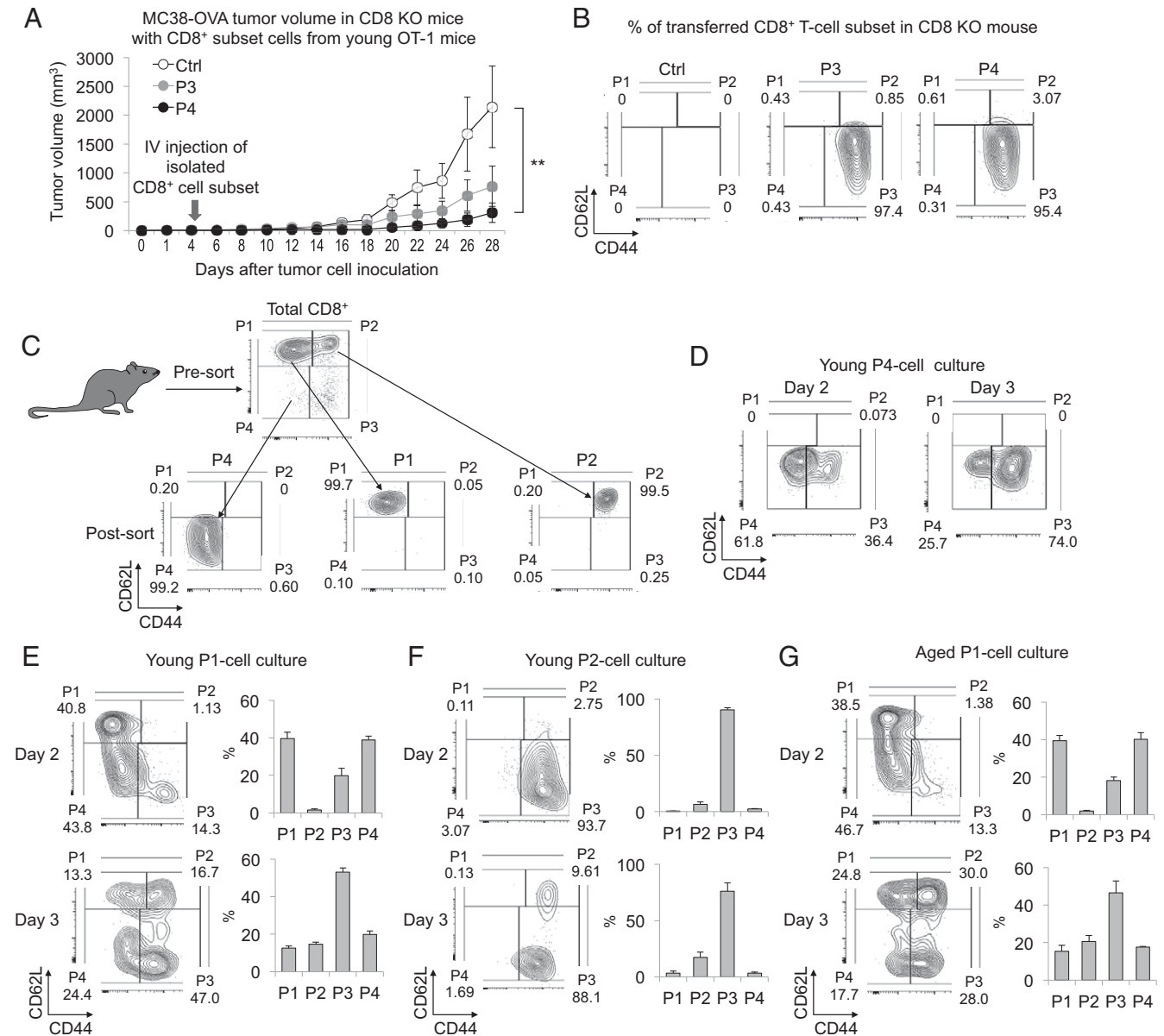


**Fig. 2.** Antitumor activity of P4 cells through differentiation to P3 cells. (A and B) To obtain the OT-1 P3 and P4 subsets, MC38-OVA cells were i.v. injected into young OT-1 mice and each subset was isolated from splenocytes. The P3 or P4 subset cells were adoptively transferred into CD8 KO mice 5 d after MC38-OVA i.d. injection. (A) Tumor volume in MC38-OVA-bearing CD8 KO mice with or without (Ctrl) the transfer of P3 or P4 cells. (B) FACS analysis of the transferred CD8<sup>+</sup> T cell subsets in peripheral blood on day 11. P1 to P4 subsets were defined by CD44 and CD62L positivity after gating on CD8<sup>+</sup> T cells. (C) Scheme of CD8<sup>+</sup> T cell subset isolation from splenocytes of young PD-1 KO mice. (D–G) FACS analysis of cultured P4 (D), P1 (E and G), or P2 (F) cells isolated from young (2–3 mo old) or aged (16–18 mo old) PD-1 KO mice 2 or 3 d after the stimulation using anti-CD3/CD28 mAbs and IL-2. Representative plots showing CD44 and CD62L expression in the indicated culture cells and percentage of CD8<sup>+</sup> T cell subsets. Data are presented as the mean ± SEM (n = 3–5); \*\*P < 0.01 (one-way ANOVA followed by Tukey’s test).

be important for the antitumor activity observed with PD-1 blockade or deficiency.

**P4 Cells Are Intermediates between P1 and P3 Cells and Have the Potential of Antitumor Activity.** To examine whether the attenuated P4 cell induction is related to the resistance to PD-1 blockade therapy in aged mice, we characterized the functional properties of the CD8<sup>+</sup> P4 subset. We first investigated the antitumor activity of P4 cells by injecting isolated P4 cells into young tumor-bearing CD8 KO mice. P3 cells were used as a positive control of effector cells. To avoid TCR repertoire bias, we used young TCR-transgenic OT-1 mice, whose CD8<sup>+</sup> T cells express a unique TCR specifically responsive to the ovalbumin (OVA) peptide. P3 and P4 subsets of CD8<sup>+</sup> T cells were induced by intravenous (i.v.) injection of OVA-expressing MC38 tumor cells (MC38-OVA) into OT-1 mice and isolated from spleen 5 d later. The same number of P3 or P4 cells was adoptively transferred into young CD8 KO mice bearing MC38-OVA. MC38-OVA growth was strongly suppressed in the mice transferred with either P3 or P4 cells (Fig. 2A). Notably, all of the transferred P4 cells had differentiated into P3 cells in the peripheral blood 6 d after the infusion (Fig. 2B). These results indicate that P4 cells have the potential to reject tumors by differentiating into P3 cells.

Although P1 and P2 cells are known to differentiate into P3 cells during activation (36, 37), P4 cells have not been well characterized because of their scarcity. To determine from which subsets P4 cells originate and to which subsets they differentiate, P1, P2, and P4 cells were isolated from young PD-1 KO mice and stimulated *in vitro* with anti-CD3/CD28 monoclonal antibodies (mAbs) and IL-2 (Fig. 2C). In agreement with the *in vivo* study, isolated P4 cells exclusively differentiated to P3 cells under these conditions (Fig. 2D). Next, we investigated whether P4 cells are generated from P1 or P2 cells. As shown in Fig. 2E and F, P4 cells were generated from P1 cells but not P2 cells 2 d after *in vitro* stimulation. These results indicate that stimulated naive P1 CD8<sup>+</sup> T cells give rise to P4 cells that further differentiate into P3 cells. Since the *in vivo* studies indicate that P4 cell induction is defective in aged mice (Fig. 1C and D), we tested the potential of aged P1 cells to generate P4 cells *in vitro*. Surprisingly, P4 and P3 cells were induced as efficiently from aged P1 cells as from young P1 cells following culture with anti-CD3/CD28 mAbs and IL-2 (Fig. 2G). These findings indicate that P1 cells from aged mice can be induced to differentiate into P4 cells by a strong *in vitro* TCR stimulant such as anti-CD3/CD28 mAbs but not by nominal antigenic stimulation.

**One-Carbon Metabolism-Related Genes Are Highly Expressed in P4 Cells.** To understand the role of P4 cells in antitumor activity in aged mice, we compared the gene expression profiles among CD8<sup>+</sup> T cell subsets (P1, P2, P3, and P4) in young PD-1 KO mice. Hierarchical clustering of global gene expression showed that each subset of CD8<sup>+</sup> T cells has a distinct gene expression profile (Fig. 3A). Genes expressed in activated T cells (such as *Ctla4*, *Prdm1*, and *Il2rb*) were more highly expressed in P4 cells than in their precursor P1 cells (Fig. 3B). In contrast, genes expressed in differentiated T cells (such as *Il7r*, *Ifng*, and *Tbx21*) were expressed at lower levels in P4 cells than in P2 or P3 cells (Fig. 3B). These results indicate that P4 cells are in an activated but premature state and distinct from more differentiated subsets of CD8<sup>+</sup> T cells such as P2 and P3 cells, supporting our hypothesis that P4 cells are pre-effector-like cells derived from naive P1 cells.

Next, gene ontology enrichment analysis was applied to determine which biological processes were up-regulated in these CD8<sup>+</sup> T cell subsets. In P4 cells, the most significantly up-regulated processes were related to 1C metabolic pathways that mediate the interconversion of serine, glycine, and folate derivatives (Fig. 3C and D). The expression of 1C-metabolism-related genes was highest in P4 cells, as shown by microarray analysis and qPCR (Fig. 3E and F). These results indicate that 1C-metabolic pathways

are selectively up-regulated in P4 cells during CD8<sup>+</sup> T cell differentiation.

Tumor inoculation increased the expression of 1C-metabolism-related genes in the total population of CD8<sup>+</sup> T cells in young WT and PD-1 KO mice (Fig. 3G), which could be explained by the generation of P4 cells (Fig. 1C and *SI Appendix*, Fig. S1C). Consistent with the higher efficiency of P4 cell induction in PD-1 KO mice (Fig. 1C and *SI Appendix*, Fig. S1C), the CD8<sup>+</sup> T cells of young PD-1 KO mice expressed higher levels of most of the 1C-metabolism-related genes than did those of young WT mice in response to MC38 tumor cell inoculation (Fig. 3G). In contrast, expression of these genes in the total CD8<sup>+</sup> T cells from aged mice did not markedly change upon tumor inoculation, regardless of genotype. The level of 1C-metabolism-related gene expression in the total CD8<sup>+</sup> T cell population thus appears to correlate with the percentage of P4 cells.

Elevated mitochondrial function is critically involved in CD8<sup>+</sup> T cell activation during the immune response (38, 39). Because P4 cells exhibited increased expression of *Shmt2*, a regulator of mitochondrial tRNA modification (33, 34) (Fig. 3E and F), we suspect that up-regulation of 1C metabolism may increase antitumor activity in part through increasing mitochondrial function. To examine mitochondrial activity in young and aged mice, we compared the oxygen consumption rate (OCR) in total CD8<sup>+</sup> T cells between tumor-bearing young and aged mice. Aged CD8<sup>+</sup> T cells from WT or PD-1 KO mice showed clear deficits in the OCR, with substantial loss of basal respiration and spare respiratory capacity (Fig. 3H and I). Together, these results suggest that defective P4 cell induction in aged mice may contribute to the reduced mitochondrial function in the CD8<sup>+</sup> T cell population, possibly through inefficient up-regulation of 1C-metabolic pathways.

**Elevated CD45RB Expression in Aged Mice.** Since P4 cells were shown to be generated from P1 cells by *in vitro* stimulation, we suspected that the lower level of P4 cell induction upon tumor inoculation observed in aged mice could be caused by inefficient transduction of TCR signals in aged P1 cells. To examine the relationship between TCR signaling and P4 cell generation, we infused MC38-OVA into OT-1 mice. The percentage of P4 cells in PLNs was markedly increased by this infusion in young but not aged OT-1 mice (Fig. 4A and B). To evaluate TCR signal transduction, we investigated the phosphorylation of ZAP-70, critical to TCR signaling (40), in total CD8<sup>+</sup> T cells from young and aged OT-1 mice after MC38-OVA infusion. MC38-OVA injection increased the percentage of CD8<sup>+</sup> T cells expressing phosphorylated ZAP-70 (p-ZAP-70) in young but not aged OT-1 mice (Fig. 4C), suggesting that antigen-stimulated TCR signaling is inhibited in aged OT-1 mice. Notably, no significant difference was observed in the intensity of the OVA-specific MHC tetramer, indicating that the TCR expression levels and/or avidity of young and aged OT-1 T cells were similar (*SI Appendix*, Fig. S4A and B). Therefore, the observed inhibition of antigen-stimulated TCR signaling in aged OT-1 mice must involve a mechanism other than TCR and MHC/antigen interaction.

Because the response of naive CD8<sup>+</sup> T cells to TCR stimulation is weaker in cells with a high density of cell surface CD45 (26), we investigated the expression level of CD45RB, the major CD45 isoform in mouse naive and memory T cells. CD45RB expression in total CD8<sup>+</sup> T cells was significantly higher in aged than in young OT-1 mice (Fig. 4D). The effect of aging on CD45RB expression was greater in P1 and P4 cells than in P2 or P3 cells (Fig. 4D). Similarly, the greatest increase in CD45RB expression was observed in P1 cells of aged WT and PD-1 KO mice (*SI Appendix*, Fig. S5A and B), suggesting that the inhibition of P4 cell induction very likely results from increased CD45RB expression in P1 cells. Increment of CD45RB expression was not observed in CD4<sup>+</sup> P1 (CD44<sup>low</sup>CD62L<sup>high</sup>) cells of aged WT and PD-1 KO mice (*SI Appendix*, Fig. S5C and D).

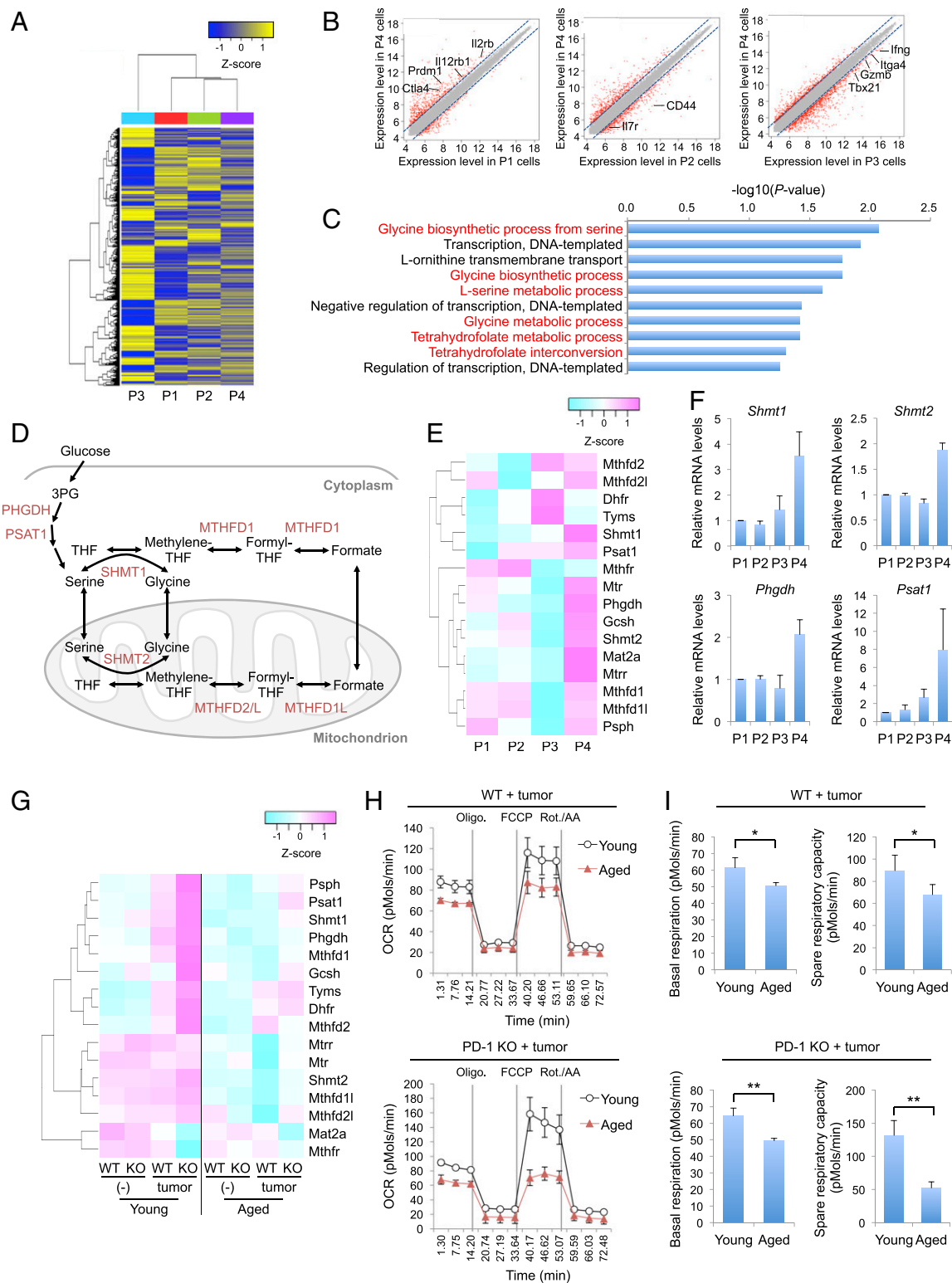


**Fig. 3.** Increased expression of 1C-metabolism-related genes in P4 cells. (A–E) Microarray analysis of P1, P2, P3, and P4 cells sorted from young PD-1 KO mice (1–3 mo old; nine mice pooled). (A) Hierarchical clustering heat map of all detected genes. (B) Scatter plots represent normalized log intensities of individual probes. The dashed lines indicate log 2-fold change. Genes previously linked to CD8<sup>+</sup> T cell activation and differentiation are listed. (C) Top 10 enriched gene ontology (GO) terms from the up-regulated genes in P4 cells. GO terms related to 1C metabolism are highlighted in red. (D) Schematic of 1C-metabolic pathways. THF, tetrahydrofolate. (E) Heat map showing the expression of 1C-metabolism-related genes in CD8<sup>+</sup> T cell subsets from splenocytes of young PD-1 KO mice. (F) Relative mRNA expression of 1C-metabolism-related genes in CD8<sup>+</sup> T cell subsets from splenocytes of young PD-1 KO mice. (G) Microarray analysis of WT or PD-1 KO CD8<sup>+</sup> T cells in PLNs or DLNs of young (2 mo old, three mice pooled) or aged (17 mo old, six mice pooled) mice with or without MC38 tumors (day 9). Heat map showing the expression of 1C-metabolism-related genes in the indicated cells. (H and I) Oxygen consumption rate (OCR) of WT or PD-1 KO CD8<sup>+</sup> T cells from DLNs of young (2–3 mo old) or aged (15–19 mo old) mice was measured using a Seahorse XFe96 analyzer. OCR trace (H) and basal respiration and spare respiratory capacity were calculated from OCR values (I). \**P* < 0.05; \*\**P* < 0.01 (two-tailed unpaired Student's *t* test). Data are presented as the mean ± SEM (*n* = 4).

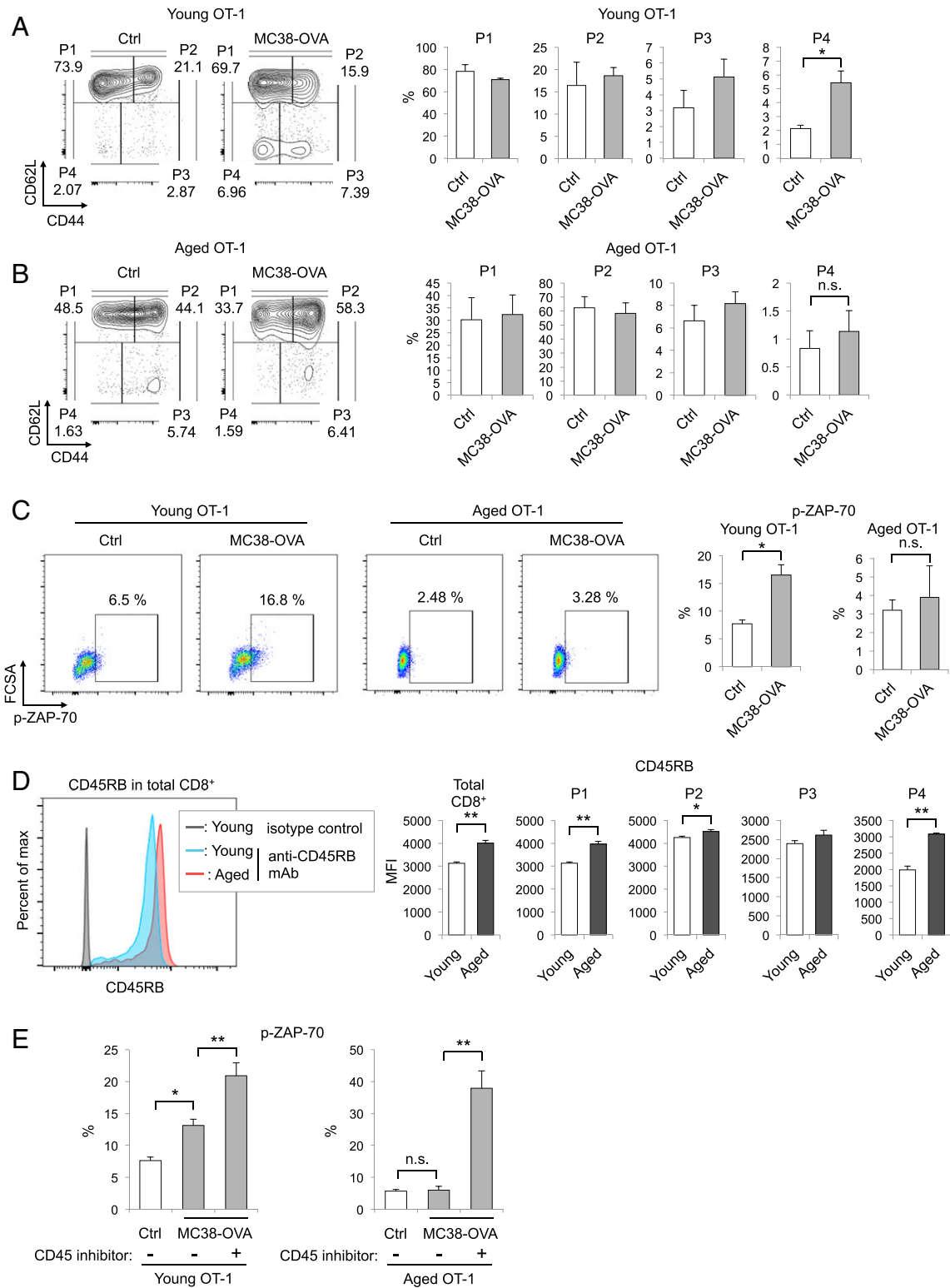


**Fig. 4.** P4 cell induction in aged CD8<sup>+</sup> T cells is attenuated by TCR signal suppression through high CD45RB expression. (A and B) Analysis of CD8<sup>+</sup> T cell subsets in PLNs of young (2–3 mo old) (A) or aged (12–15 mo old) (B) OT-1 mice with or without i.v. injection of MC38-OVA cells. Representative plots showing CD44 and CD62L expression on CD8<sup>+</sup> T cells and the percentage of each CD8<sup>+</sup> T cell subset in the indicated mice 5 d after MC38-OVA injection. (C) The percentages of pZAP70<sup>+</sup> CD8<sup>+</sup> T cells in PLNs from young or aged OT-1 mice with or without MC38-OVA injection are shown in representative plots. (D) CD45RB expression levels in total CD8<sup>+</sup> T cells or each subset from PLNs of young (2–3 mo old) or aged (14–17 mo old) OT-1 mice are shown in representative plots. (E) CD8<sup>+</sup> T cells were isolated from PLNs of young or aged OT-1 mice and cultured with or without MMC-treated MC38-OVA cells for 1 d. In the last 1 h, vehicle or CD45 inhibitor (0.05  $\mu$ M) was added. The graphs show the percentages of p-ZAP-70<sup>+</sup> cells relative to all CD8<sup>+</sup> T cells. Data are represented as the mean  $\pm$  SEM ( $n = 3-6$ ). \* $P < 0.05$ ; \*\* $P < 0.01$ ; n.s., not significant (one-way ANOVA followed by Tukey's test or two-tailed unpaired Student's  $t$  test).

To next test whether CD45RB expression suppresses CD8<sup>+</sup> T cell activation by downregulating TCR signal transduction, we evaluated the phosphorylation of ZAP-70 in OT-I CD8<sup>+</sup> T cells after treatment with a CD45-specific inhibitor (41). Consistent with the in vivo results (Fig. 4C), the percentage of p-ZAP-70<sup>+</sup> CD8<sup>+</sup> T cells was increased by coculture with MC38-OVA cells in young but not aged CD8<sup>+</sup> T cells (Fig. 4E). Under this condition, the addition of a CD45 inhibitor increased p-ZAP-70<sup>+</sup> cell induction in aged as well as young CD8<sup>+</sup> T cells. These data indicate that age-related inefficiency in tumor rejection is likely due to increased expression of CD45RB in aged CD8<sup>+</sup> T cells.

**Xenogeneic Cell Treatment Increases P4 Cell Induction and Ameliorates the Antitumor Capacity of CD8<sup>+</sup> T Cells in Aged Mice.** Since the suppression of P1-to-P4 transition in aged mice can be recovered by strong in vivo stimulation as shown above, we investigated whether strong stimulation using xenogeneic cells (human Burkitt lymphoma, Daudi cells) could recover P4 CD8<sup>+</sup> T cell induction in aged PD-1 KO mice (Fig. 5A). Ten days after Daudi cell i.v. injection (day 0: before MC38 tumor inoculation), the percentage of P4 cells but not P1–P3 cells was markedly increased in PLNs of both young and aged PD-1 KO mice (Fig. 5B). As expected, the expression levels of genes related to 1C metabolism in CD8<sup>+</sup> T cells from aged PD-1 KO mice were increased by the Daudi cell injection (Fig. 5C). Consistent with these findings, Daudi cell injection reduced CD45RB expression in the P1 cells of aged PD-1 KO mice (Fig. 5D).

Daudi cell injection dramatically inhibited MC38 tumor growth in aged PD-1 KO mice and increased their survival (Fig. 5E and F). Age-related unresponsiveness to anti-PD-L1 mAb in WT mice was also recovered by the Daudi cell treatment (SI Appendix, Fig. S6 A–E). On day 6 after tumor inoculation, the percentage of p-ZAP-70–positive cells was augmented in aged PD-1 KO mice treated with Daudi cell injection (Fig. 5G), suggesting that xenogeneic stimulation augments the TCR signals for tumor antigens. We further investigated whether Daudi cell treatment increases the proliferation of tumor antigen-reactive CD8<sup>+</sup> T cells. MC38-OVA cells were inoculated into PD-1 KO mice 10 d after Daudi cell injection. Then, the induction of P4 cells and the emergence of OVA tetramer<sup>+</sup> CD8<sup>+</sup> T cells were monitored. Six days after MC38-OVA inoculation, P4 cell percentage was increased by Daudi cell injection in DLNs of aged PD-1 KO mice (SI Appendix, Fig. S7A). In tumor sites, the percentage of P1 and P4 cells was very low, and most tumor-infiltrating CD8<sup>+</sup> T cells were already differentiated into P3 subset (more than 85%) (SI Appendix, Fig. S7B). On the other hand, the percentage of OVA tetramer<sup>+</sup> CD8<sup>+</sup> T cells was elevated in DLNs and tumor sites in aged PD-1 KO mice bearing MC38-OVA by the injection of Daudi cells (Fig. 5H and I). These results indicate that this treatment enhances the differentiation of antigen-specific CD8<sup>+</sup> T cells from naive to effector CD8<sup>+</sup> T cells in the secondarily lymphoid organs, and thereby increases infiltration of antigen-specific CD8<sup>+</sup> T cells in tumors (42, 43). Given that prestimulation with Daudi cells boosts P4 cell induction and 1C metabolism in the CD8<sup>+</sup> T cells of aged mice, it was reasonable that Daudi cell injection increased both the basal respiration and spare respiratory capacity of aged CD8<sup>+</sup> T cells in DLNs (SI Appendix, Fig. S8 A–C). Injection of splenocytes from Balb/c mice as alloantigens also increased the antitumor effects of PD-1 blockade therapy in aged WT mice (SI Appendix, Fig. S9 A–D). We also tested the effect of Daudi cell injection on CD8<sup>+</sup> T cell responses in WT mice after MC38 tumor cell inoculation. Five days after the MC38 cell inoculation, young and aged WT mice were injected with Daudi cells and anti-PD-L1 antibody. Two days after the Daudi cell administration, the percentage of P4 cells was increased in aged WT mice with anti-PD-L1 mAb treatment (SI Appendix, Fig. S10A). In addition, the percentage of p-ZAP-70–positive cells in DLNs and the number of tumor-infiltrating CD8<sup>+</sup> T cells were also augmented with Daudi

cell administration in aged WT mice (SI Appendix, Fig. S10 B and C). These data suggest that strong immune stimulation by the xenogeneic or allogeneic cell treatment rescued the compromised antitumor response of CD8<sup>+</sup> T cells in aged mice and recovered the antitumor effects of PD-1 deficiency or PD-1 blockade therapy. Together, these findings show that strong immune stimulation by nonself cells can rescue the insufficient antitumor response in aged mice through the recovery of TCR signal transduction and induction of the P4 subset, which increases the efficacy of PD-1 deficiency and blockade therapy.

## Discussion

Aged individuals and animals are known to be insensitive to immunotherapy because of age-related suppression of CD8<sup>+</sup> T cell responses (9–11). The mechanism underlying suppression of the CD8<sup>+</sup> T cell response to tumor antigen is largely unknown. We found that aged tumor-bearing mice had significantly fewer P4 cells, a poorly characterized subset of CD44<sup>low</sup>CD62L<sup>low</sup> CD8<sup>+</sup> T cells, due to weakened TCR signaling caused by an increase in CD45RB expression. The P4 subset differentiates from the naive P1 subset and further matures into the effector/memory subset (P3) critical to antitumor activity (44, 45). The P4 subset is unique in its higher expression of 1C-metabolism–related genes, which are associated with the growth and survival of proliferating cells and involved in CD8<sup>+</sup> T cell differentiation (29, 32, 46, 47). These aging-induced defects in CD8<sup>+</sup> T cell differentiation and the efficacy of PD-1 blockade therapy were recovered by strong immunogenic stimulation using nonself cells.

Age-associated deviations in the naive T cell repertoire have been proposed as the main reason for the suppression of T cell responses in aged individuals (48, 49). However, we found that OT-1 transgenic mice, in which all CD8<sup>+</sup> T cells carry the OVA-specific TCR, became insensitive to the specific antigen on tumor cells with aging. Our study further revealed that strong TCR stimulation in vitro or with xenogeneic cell treatment in vivo recovered P4 cell generation, which should be difficult if P4 cell deficiency was due to the lack of TCR repertoire. In a similar line, an impaired antitumor response observed in aging OT-II CD4<sup>+</sup> T cells, which express an OVA-specific TCR, is caused by impaired Th1 differentiation resulting from the IL-6–enriched environment that comes with aging (50). These results indicate that repertoire limitation is unlikely to be the major cause of suppression of the T cell response in aged animals.

Previous studies report that TCR signaling becomes suppressed with aging, leading to impaired T cell responses (51, 52). The levels of p-ZAP-70 induced by T cell activation are reported to be lower in aged humans and mice (53, 54). Consistent with these reports, we also found that ZAP-70 phosphorylation was lower in aged mice with tumor cells. Our data showed that this change was caused by an increase in CD45RB expression in aged P1 cells. CD45 negatively regulates TCR signaling by dephosphorylating tyrosine 394 of the Lck tyrosine kinase, leading to suppression of ZAP-70 activation (55). Indeed, the induction of p-ZAP-70<sup>+</sup> CD8<sup>+</sup> T cells was recovered by treatment with a CD45 inhibitor. These results strongly support the hypothesis that suppression of CD8<sup>+</sup> T cell responses in aged animals is caused by deficient TCR signaling in naive T cells via the increased expression of CD45RB.

A large number of T cells are activated by TCR stimulation through the interaction with allogeneic or xenogeneic MHC molecules, either directly (e.g., donor MHC presenting donor peptides) or indirectly (e.g., recipient MHC presenting donor peptides) (56–58). We speculate that P4 cell recovery in aged mice is mediated by TCR recognition of nonself antigens. Since the TCR recognizes a broad range of different peptides in nature (59, 60), the recovered P4 cells or the preactivated P1 cells by nonself antigens cross-react to tumor antigens, leading to an increase in antitumor responses. In addition, allogeneic or xenogeneic antigens can activate CD8<sup>+</sup> T cells through antigen-presenting cell (APC)

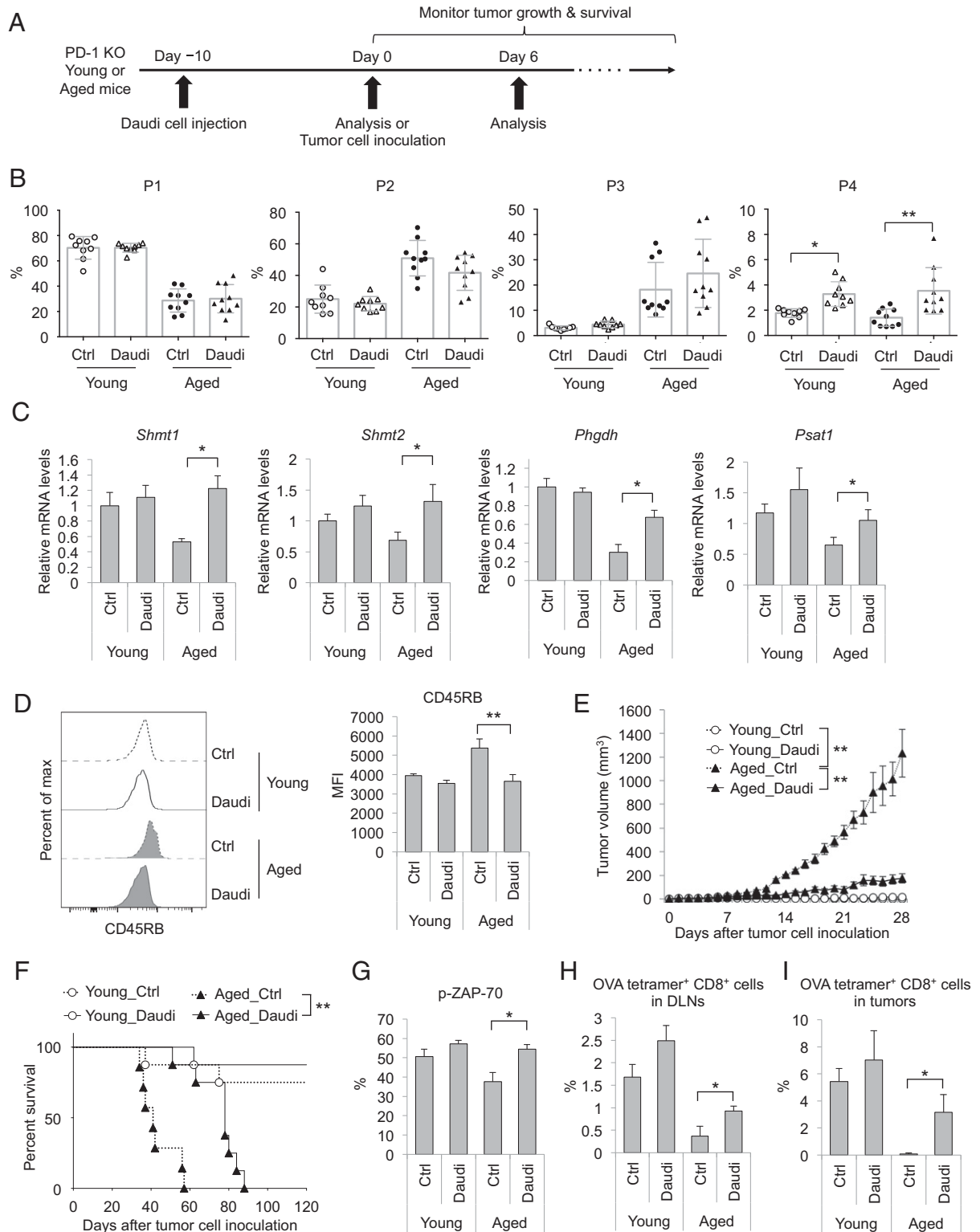


**Fig. 5.** Recovery of P4 cell induction and antitumor activity in aged mice by xenogeneic cell injection. (A) Schematic diagram of the experimental schedule. (B–D) Young (3–4 mo old) and aged (16–18 mo old) PD-1 KO mice were i.v. injected with Daudi cells (day –10). Ten days after injection (day 0), PLN cells of the mice were analyzed by FACS and real-time PCR. (B) Percentages of P1–P4 subsets relative to all CD8<sup>+</sup> T cells in PLNs. (C) Expression levels of 1C-metabolism-related genes in CD8<sup>+</sup> T cells. (D) CD45RB expression levels in P1 cells from PLNs. (E–I) Young (3–4 mo old) and aged (17–18 mo old) PD-1 KO mice were i.v. injected with or without (Ctrl) Daudi cells (day –10). Ten days after the transfer (day 0), the mice were i.d. inoculated with MC38 (E–G) or MC38-OVA (H and I) cells and used for the following experiments. MC38-tumor sizes (E) and percent survival (F). (G) The percentage of p-ZAP-70<sup>+</sup> cells relative to all CD8<sup>+</sup> T cells from DLNs on day 6. (H and I) Frequency of OVA tetramer<sup>+</sup> CD8<sup>+</sup> T cells in DLNs (H) or tumor tissues (I) on day 6. Data are presented as the mean ± SEM (n = 9–10 for B; n = 4–6 for C–I). \*P < 0.05; \*\*P < 0.01 (one-way ANOVA followed by Tukey's test, log-rank test, or two-tailed unpaired Student's t test).



activation and their cytokine production (61, 62). Recent reports indicate that cytokines induce specific subsets, such as “bystander” CD8<sup>+</sup> T cells, which recognize a wide range of antigens (63, 64). These suggest the possibility that cytokines produced by nonself cell treatment may be involved in the recovery of P4 cells and antitumor responses.

Nevertheless, the regulation mechanism of CD45RB expression by aging and strong immunogenic stimulation using nonself cells remains unclear. In aged individuals and animals, it is known that homeostatic proliferation of naive T cells is driven by the MHC with self-peptides and homeostatic cytokines (23). Previous report showed that memory CD8<sup>+</sup> T cells induced by high-affinity TCR priming had lower CD45RB expression than that in low-affinity-primed memory CD8<sup>+</sup> T cells (65). Interaction between TCR and allogeneic MHC or allo-pMHC is much stronger than that of TCR and self-pMHC because of no experience of negative selection in thymus (66). Therefore, a weak TCR/self-pMHC interaction in aged P1 cells may increase CD45RB expression, which is down-regulated by strong interaction between TCR and MHC presenting nonself antigens. Further study will be required to reveal the molecular mechanism by which CD45RB expression is regulated by aging and nonself cell treatment.

## Materials and Methods

**Mice and Cells.** Mice were maintained under specific pathogen-free conditions at the Institute of Laboratory Animals, Graduate School of Medicine, Kyoto University, or RIKEN Center for Integrative Medical Sciences. All animal experiments were performed according to the guidelines approved by the respective institutional review boards. PD-1<sup>-/-</sup> (PD-1 KO) mice were described previously (67). C57BL/6N WT mice were purchased from Charles River Laboratories Japan or Shimizu Laboratory Supplies Japan. OT-1 TCR-transgenic and CD8<sup>-/-</sup> (CD8 KO) mice were purchased from The Jackson Laboratory (originally from M. B. Bevan at University of Washington [Seattle, WA], or T. Mak at University of Toronto [Toronto, ON, Canada]). The murine colon adenocarcinoma (MC38) cell line was kindly provided by J. P. Allison, Memorial Sloan-Kettering Cancer (New York, NY), and the MC38 cell line expressing ovalbumin (OVA) (MC38-OVA) was generated by transducing MC38 cells with pMXs-based OVA-F2A-EGFP retrovirus. The information of the murine glioblastoma cell line (GL261) was previously described (68). Cells were maintained in RPMI 1640 (Gibco; 11875-093) or DMEM (Gibco; 11995-065) supplemented with 10% heat-inactivated fetal bovine serum (FBS) and penicillin–streptomycin (Nacal Tesque; 26253-84) and free of mycobacterial infection.

**Mouse Therapy Model and Nonself Cell Treatment.** MC38 cells ( $5 \times 10^5$  or  $2 \times 10^6$ ) or GL261 ( $5 \times 10^5$ ) were intradermally (i.d.) injected into the right flank of mice (day 0). Tumor-inoculated mice were intraperitoneally injected with anti-PD-L1 mAb (clone 1-111A.4) (6 mg/kg) 5 d after tumor inoculation (day 5). The therapy was repeated three times every 6 d (days 5, 11, and 17). An isotype of anti-PD-L1 mAb (rat IgG2a) was used as a control. Tumor growth was monitored by measuring the tumor size using calipers and the volume calculated using the formula for a typical ellipsoid:  $\pi$  (length  $\times$  breadth  $\times$  height)/6. Nonself cell treatment was performed 10 d before or 5 d after tumor cell inoculation by i.v. injection of human Burkitt’s lymphoma Daudi cells or mitomycin C (MMC)-treated splenocytes ( $2 \times 10^6$  cells/mouse) from BALB/c mice or C57BL/6N mice as a control.

**Primary Cell Isolation for Analysis and Culture.** PLN and DLN cells and tumor-infiltrating lymphocytes were isolated as previously described (39). For splenocyte analysis, spleens were briefly lysed and suspended in ammonium chloride potassium buffer to lyse red blood cells. The splenocytes were washed and resuspended in RPMI medium 1640 supplemented with 10% FBS, L-glutamine, 55  $\mu$ M 2-mercaptoethanol, penicillin–streptomycin, 1 mM sodium pyruvate (Gibco), and 1% MEM NEAA (Gibco) (T cell medium). We further isolated subsets of CD8<sup>+</sup> T cells using CD8a (Ly-2) micro beads (Miltenyi Biotec; 130-117-044) and FACSAria (BD Biosciences). For peripheral blood cell analysis, collected peripheral blood cells were treated with ammonium chloride potassium buffer and washed with T cell medium. Purified cells were stimulated with anti-CD3/CD28 Dynabeads (Gibco) and recombinant human IL-2 (20 U/mL; PeproTech) in T cell medium. To stimulate CD8<sup>+</sup> T cells using MC38-OVA cells, CD8<sup>+</sup> T cells isolated from LNs of OT-1 mice were cocultured with the MMC-treated MC38-OVA cells in T cell medium. One day after stimulation, the cells were treated with 0.05  $\mu$ M CD45 inhibitor VI (EMD Millipore) for 1 h.

**Flow Cytometry Analysis.** The following mAbs were used to detect the indicated antigens: CD3 (145-2C11), CD8 (53-6.7), and phospho-ZAP70/Syk (n3koku5) from Invitrogen; CD44 (IM7), and CD62L (MEL-14) from TONBO Biosciences or BioLegend; CD8 (KT15) from MBL Life Science; and CD45RB (16A), and CD4 (RM4-4) from BD Pharmingen. H-2Kb-Negative (SIY) Tetramer-SIYRYL-APC (TS-5001-2C) and H-2Kb OVA Tetramer-SIINFELK-APC (TS-M008-2) were obtained from MBL Life Science. Flow cytometry experiments were performed using a FACSCanto II or LSRFortessa X-20 (BD Biosciences) and analyzed using FlowJo software (FlowJo).

**CD8 KO and OT-1 Mouse Model.** To induce P3 and P4 cells, MC38-OVA cells ( $1-2 \times 10^6$ ) were i.v. injected into OT-1 mice. After 5 d, P3 and P4 cells were isolated from those mice. Each isolated CD8<sup>+</sup> T cell subset was i.v. injected into CD8 KO mice that had been i.d. injected with  $2 \times 10^5$  MC38-OVA cells 5 d before CD8<sup>+</sup> T cell infusion. Peripheral blood was obtained 6 d after the infusion to analyze infused cell differentiation.

**Microarray Analysis.** Total RNA was extracted from total CD8<sup>+</sup> T cells pooled from three to six mice (per group) or from the CD8<sup>+</sup> T cell subset pooled from nine mice (per group) using Nucleospin RNA (Macherey-Nagel) according to the manufacturer’s protocols. Microarray analysis was performed by MacroGen using the Mouse 8  $\times$  60K v2 Microarray (Agilent Technologies). The data were deposited in the Gene Expression Omnibus (GEO) repository (<https://www.ncbi.nlm.nih.gov/geo/>) under the accession nos. GSE161659 and GSE161660. Gene ontology enrichment analysis was performed using the Database for Annotation, Visualization, and Integrated Discovery (DAVID) (<https://david.abcc.ncifcrf.gov/>). Differentially expressed genes were visualized using R 3.1.2 or RStudio, version 1.1.383.

**Real-Time PCR.** Total RNA was isolated from cells using Nucleospin RNA (Macherey-Nagel) and used for cDNA synthesis using Revatrac reverse transcriptase (Toyobo) and random primer generation according to the manufacturer’s instructions. Real-time PCR was performed to amplify the indicated mRNAs using the Applied Biosystems 7500 Fast Real-Time PCR system (ABI) and PowerUp SYBR Green Master Mix (Applied Biosystems). The expression level of each gene was normalized to the mRNA level of  $\beta$ -actin. The primer sequences were as follows: *Shmt1* forward (Fw), 5'-CCAGAGTGC-TGTGGCAACTC-3'; *Shmt1* reverse (Rv), 5'-GCAAACACAGGCTGTCTC-3'; *Shmt2* Fw, 5'-GACAGTTGAGGACACTGGC-3'; *Shmt2* Rv, 5'-CCAGAGAGG-AGTGACATCTC-3'; *Phgdh* Fw, 5'-TGGCTCTCGCAGAAATTGGAAG-3'; *Phgdh* Rv, 5'-TGTCATTCAGCAAGCCTGTGGT-3'; *Psat1* Fw, 5'-GATGAACATCCCATTCGCATTGG-3'; *Psat1* Rv, 5'-GCGTTATACAGAGAGGACGCAATG-3';  $\beta$ -actin Fw, 5'-TAAGGCCAACCGTGAAG-3'; and  $\beta$ -actin Rv, 5'-GAGGCATACAGG-GACAGCAC-3'.

**OCR Analysis.** OCR assay was performed as described previously (39), with minor modifications. OCR of CD8<sup>+</sup> cells isolated from DLNs was measured on an XFe96 Extracellular Flux analyzer (Agilent Technologies) using the Seahorse XFe96 Extracellular Flux assay kit and Seahorse XF Cell Mito Stress test kit (Agilent Technologies). CD8<sup>+</sup> cells ( $3 \times 10^5$  per well) were seeded in Cell-Tak (Corning)-coated XFe96 plates. The spare respiratory capacity was calculated from the OCR graph as described previously (69). The basal respiration was calculated by subtracting the nonmitochondrial respiration (the value after rotenone/antimycin A addition from the value before oligomycin addition) (70).

**Statistical Analysis.** Data were analyzed using Prism 7 (GraphPad), and the results are presented as the mean  $\pm$  SEM. Comparisons of two groups were analyzed using unpaired two-tailed Student’s *t* test; comparisons of more than two groups were analyzed using one-way analysis of variance (ANOVA) followed by Tukey’s multiple-comparison tests. Survival rates were evaluated using the Kaplan–Meier method, and statistical significance was determined by log rank test.

**Data Availability.** All microarray data have been deposited in the National Center for Biotechnology Information GEO database (accession nos. GSE161659 and GSE161660).

**ACKNOWLEDGMENTS.** We sincerely thank K. Yurimoto, Y. Kitawaki, M. Al-Habsi, R. Menzies, A. Kumar, M. Akrami, R. Hatae, K. Yamasaki, and S. Delghandi for assistance with sample preparation and useful discussion. We also are grateful to S. Fagarasan and M. Miyajima for kindly providing aged WT and PD-1 KO mice. This work was supported by the Japan Agency for Medical Research and Development under Grant 20cm0106302h0005 (T.H.) and the Japan Society for the Promotion of Science KAKENHI Grant 20K07615 (Y.N.).

1. T. Finkel, M. Serrano, M. A. Blasco, The common biology of cancer and ageing. *Nature* **448**, 767–774 (2007).
2. K. Tomihara, T. J. Curiel, B. Zhang, Optimization of immunotherapy in elderly cancer patients. *Crit. Rev. Oncog.* **18**, 573–583 (2013).
3. S. L. Topalian *et al.*, Safety, activity, and immune correlates of anti-PD-1 antibody in cancer. *N. Engl. J. Med.* **366**, 2443–2454 (2012).
4. A. Ribas *et al.*, Association of pembrolizumab with tumor response and survival among patients with advanced melanoma. *JAMA* **315**, 1600–1609 (2016).
5. M. Reck *et al.*; KEYNOTE-024 Investigators, Pembrolizumab versus chemotherapy for PD-L1-positive non-small-cell lung cancer. *N. Engl. J. Med.* **375**, 1823–1833 (2016).
6. P. S. Chowdhury, K. Chamoto, T. Honjo, Combination therapy strategies for improving PD-1 blockade efficacy: A new era in cancer immunotherapy. *J. Intern. Med.* **283**, 110–120 (2018).
7. W. Zou, J. D. Wolchok, L. Chen, PD-L1 (B7-H1) and PD-1 pathway blockade for cancer therapy: Mechanisms, response biomarkers, and combinations. *Sci. Transl. Med.* **8**, 328rv4 (2016).
8. A. L. Shergold, R. Millar, R. J. B. Nibbs, Understanding and overcoming the resistance of cancer to PD-1/PD-L1 blockade. *Pharmacol. Res.* **145**, 104258 (2019).
9. J. Brahmer *et al.*, Nivolumab versus docetaxel in advanced squamous-cell non-small-cell lung cancer. *N. Engl. J. Med.* **373**, 123–135 (2015).
10. C. Helissey, C. Vicier, S. Champiat, The development of immunotherapy in older adults: New treatments, new toxicities? *J. Geriatr. Oncol.* **7**, 325–333 (2016).
11. Á. Padrón *et al.*, Age effects of distinct immune checkpoint blockade treatments in a mouse melanoma model. *Exp. Gerontol.* **105**, 146–154 (2018).
12. J. Sceneay *et al.*, Interferon signaling is diminished with age and is associated with immune checkpoint blockade efficacy in triple-negative breast cancer. *Cancer Discov.* **9**, 1208–1227 (2019).
13. K. Naylor *et al.*, The influence of age on T cell generation and TCR diversity. *J. Immunol.* **174**, 7446–7452 (2005).
14. M. Ahmed *et al.*, Clonal expansions and loss of receptor diversity in the naive CD8 T cell repertoire of aged mice. *J. Immunol.* **182**, 784–792 (2009).
15. Q. Qi *et al.*, Diversity and clonal selection in the human T-cell repertoire. *Proc. Natl. Acad. Sci. U.S.A.* **111**, 13139–13144 (2014).
16. J. Nikolich-Zugich, G. Li, J. L. Uhrlaub, K. R. Renkema, M. J. Smithey, Age-related changes in CD8 T cell homeostasis and immunity to infection. *Semin. Immunol.* **24**, 356–364 (2012).
17. M. T. Ventura, M. Casciaro, S. Gangemi, R. Buquicchio, Immunosenescence in aging: Between immune cells depletion and cytokines up-regulation. *Clin. Mol. Allergy* **15**, 21 (2017).
18. E. J. Wherry, R. Ahmed, Memory CD8 T-cell differentiation during viral infection. *J. Virol.* **78**, 5535–5545 (2004).
19. J. C. Nolz, G. R. Starbeck-Miller, J. T. Hartly, Naive, effector and memory CD8 T-cell trafficking: Parallels and distinctions. *Immunotherapy* **3**, 1223–1233 (2011).
20. J. Nikolich-Zugich, The twilight of immunity: Emerging concepts in aging of the immune system. *Nat. Immunol.* **19**, 10–19 (2018).
21. B. Youngblood, J. S. Hale, R. Ahmed, T-cell memory differentiation: Insights from transcriptional signatures and epigenetics. *Immunology* **139**, 277–284 (2013).
22. D. Sauce *et al.*, Lymphopenia-driven homeostatic regulation of naive T cells in elderly and thymectomized young adults. *J. Immunol.* **189**, 5541–5548 (2012).
23. N. Minato, M. Hattori, Y. Hamazaki, Physiology and pathology of T-cell aging. *Int. Immunol.* **32**, 223–231 (2020).
24. J. Rossy, D. J. Williamson, K. Gaus, How does the kinase Ick phosphorylate the T cell receptor? Spatial organization as a regulatory mechanism. *Front. Immunol.* **3**, 167 (2012).
25. R. J. Brownlie, R. Zamojska, T cell receptor signalling networks: Branched, diversified and bounded. *Nat. Rev. Immunol.* **13**, 257–269 (2013).
26. J. H. Cho *et al.*, CD45-mediated control of TCR tuning in naive and memory CD8<sup>+</sup> T cells. *Nat. Commun.* **7**, 13373 (2016).
27. A. C. Maue *et al.*, T-cell immunosenescence: Lessons learned from mouse models of aging. *Trends Immunol.* **30**, 301–305 (2009).
28. J. Nikolich-Zugich, Aging of the T cell compartment in mice and humans: From no naive expectations to foggy memories. *J. Immunol.* **193**, 2622–2629 (2014).
29. M. Yang, K. H. Vousden, Serine and one-carbon metabolism in cancer. *Nat. Rev. Cancer* **16**, 650–662 (2016).
30. G. S. Ducker, J. D. Rabinowitz, One-carbon metabolism in health and disease. *Cell Metab.* **25**, 27–42 (2017).
31. N. Ron-Harel *et al.*, Mitochondrial biogenesis and proteome remodeling promote one-carbon metabolism for T cell activation. *Cell Metab.* **24**, 104–117 (2016).
32. E. H. Ma *et al.*, Serine is an essential metabolite for effector T cell expansion. *Cell Metab.* **25**, 345–357 (2017).
33. R. J. Morscher *et al.*, Mitochondrial translation requires folate-dependent tRNA methylation. *Nature* **554**, 128–132 (2018).
34. D. R. Minton *et al.*, Serine catabolism by SHMT2 is required for proper mitochondrial translation initiation and maintenance of formylmethionyl-tRNAs. *Mol. Cell* **69**, 610–621.e5 (2018).
35. N. Ron-Harel *et al.*, Defective respiration and one-carbon metabolism contribute to impaired naive T cell activation in aged mice. *Proc. Natl. Acad. Sci. U.S.A.* **115**, 13347–13352 (2018).
36. C. H. June, Principles of adoptive T cell cancer therapy. *J. Clin. Invest.* **117**, 1204–1212 (2007).
37. N. S. Joshi, S. M. Kaech, Effector CD8 T cell development: A balancing act between memory cell potential and terminal differentiation. *J. Immunol.* **180**, 1309–1315 (2008).
38. N. E. Scharping *et al.*, The tumor microenvironment represses T cell mitochondrial biogenesis to drive intratumoral T cell metabolic insufficiency and dysfunction. *Immunity* **45**, 701–703 (2016).
39. K. Chamoto *et al.*, Mitochondrial activation chemicals synergize with surface receptor PD-1 blockade for T cell-dependent antitumor activity. *Proc. Natl. Acad. Sci. U.S.A.* **114**, E761–E770 (2017).
40. H. Wang *et al.*, ZAP-70: An essential kinase in T-cell signaling. *Cold Spring Harb. Perspect. Biol.* **2**, a002279 (2010).
41. M. Perron, H. U. Saragovi, Inhibition of CD45 phosphatase activity induces cell cycle arrest and apoptosis of CD45<sup>+</sup> lymphoid tumors ex vivo and in vivo. *Mol. Pharmacol.* **93**, 575–580 (2018).
42. D. S. Chen, I. Mellman, Oncology meets immunology: The cancer-immunity cycle. *Immunity* **39**, 1–10 (2013).
43. R. Ajina, D. Zamalin, L. M. Weiner, Functional genomics: Paving the way for more successful cancer immunotherapy. *Brief. Funct. Genomics* **18**, 86–98 (2019).
44. M. Sharpe, N. Mount, Genetically modified T cells in cancer therapy: Opportunities and challenges. *Dis. Model. Mech.* **8**, 337–350 (2015).
45. R. W. Jenkins, D. A. Barbie, K. T. Flaherty, Mechanisms of resistance to immune checkpoint inhibitors. *Br. J. Cancer* **118**, 9–16 (2018).
46. R. J. DeBerardinis, N. S. Chandel, Fundamentals of cancer metabolism. *Sci. Adv.* **2**, e1600200 (2016).
47. N. M. Chapman, M. R. Boothby, H. Chi, Metabolic coordination of T cell quiescence and activation. *Nat. Rev. Immunol.* **20**, 55–70 (2020).
48. E. S. Egorov *et al.*, The changing landscape of naive T cell receptor repertoire with human aging. *Front. Immunol.* **9**, 1618 (2018).
49. C. S. Palmer *et al.*, Emerging role and characterization of immunometabolism: Relevance to HIV pathogenesis, serious non-AIDS events, and a cure. *J. Immunol.* **196**, 4437–4444 (2016).
50. H. Tsukamoto, S. Senju, K. Matsumura, S. L. Swain, Y. Nishimura, IL-6-mediated environmental conditioning of defective Th1 differentiation dampens antitumor immune responses in old age. *Nat. Commun.* **6**, 6702 (2015).
51. R. A. Miller, Effect of aging on T lymphocyte activation. *Vaccine* **18**, 1654–1660 (2000).
52. G. Pawelec, K. Hirokawa, T. Fülöp, Altered T cell signalling in ageing. *Mech. Ageing Dev.* **122**, 1613–1637 (2001).
53. R. L. Whisler, M. Chen, B. Liu, Y. G. Newhouse, Age-related impairments in TCR/CD3 activation of ZAP-70 are associated with reduced tyrosine phosphorylations of zeta-chains and p59fyn/p56lck in human T cells. *Mech. Ageing Dev.* **111**, 49–66 (1999).
54. T. Fülöp Jr, A. Larbi, G. Dupuis, G. Pawelec, Ageing, autoimmunity and arthritis: Perturbations of TCR signal transduction pathways with ageing—a biochemical paradigm for the ageing immune system. *Arthritis Res. Ther.* **5**, 290–302 (2003).
55. T. Furukawa, M. Itoh, N. X. Krueger, M. Streuli, H. Saito, Specific interaction of the CD45 protein-tyrosine phosphatase with tyrosine-phosphorylated CD3 zeta chain. *Proc. Natl. Acad. Sci. U.S.A.* **91**, 10928–10932 (1994).
56. K. F. Lindahl, D. B. Wilson, Histocompatibility antigen-activated cytotoxic T lymphocytes. II. Estimates of the frequency and specificity of precursors. *J. Exp. Med.* **145**, 508–522 (1977).
57. M. Cascalho, J. L. Platt, Xenotransplantation and other means of organ replacement. *Nat. Rev. Immunol.* **1**, 154–160 (2001).
58. N. Degauque, S. Brouard, J. P. Souillou, Cross-reactivity of TCR repertoire: Current concepts, challenges, and implication for allotransplantation. *Front. Immunol.* **7**, 89 (2016).
59. L. J. D’Orsogna, D. L. Roelen, I. I. Doxiadis II, F. H. Claas, TCR cross-reactivity and allorecognition: New insights into the immunogenetics of allorecognition. *Immunogenetics* **64**, 77–85 (2012).
60. M. Hebeisen *et al.*, Molecular insights for optimizing T cell receptor specificity against cancer. *Front. Immunol.* **4**, 154 (2013).
61. S. Srivatsan *et al.*, Allogeneic tumor cell vaccines: The promise and limitations in clinical trials. *Hum. Vaccin. Immunother.* **10**, 52–63 (2014).
62. C. P. Huang, C. C. Chen, C. R. Shyr, Xenogeneic cell therapy provides a novel potential therapeutic option for cancers by restoring tissue function, repairing cancer wound and reviving anti-tumor immune responses. *Cancer Cell Int.* **18**, 9 (2018).
63. Y. Simoni *et al.*, Bystander CD8<sup>+</sup> T cells are abundant and phenotypically distinct in human tumour infiltrates. *Nature* **557**, 575–579 (2018).
64. T. S. Kim, E. C. Shin, The activation of bystander CD8<sup>+</sup> T cells and their roles in viral infection. *Exp. Mol. Med.* **51**, 1–9 (2019).
65. S. M. Krummey *et al.*, Low-affinity memory CD8<sup>+</sup> T cells mediate robust heterologous immunity. *J. Immunol.* **196**, 2838–2846 (2016).
66. N. J. Felix, P. M. Allen, Specificity of T-cell alloreactivity. *Nat. Rev. Immunol.* **7**, 942–953 (2007).
67. H. Nishimura, N. Minato, T. Nakano, T. Honjo, Immunological studies on PD-1 deficient mice: Implication of PD-1 as a negative regulator for B cell responses. *Int. Immunol.* **10**, 1563–1572 (1998).
68. A. Kumar, K. Chamoto, P. S. Chowdhury, T. Honjo, Tumors attenuating the mitochondrial activity in T cells escape from PD-1 blockade therapy. *eLife* **9**, e52330 (2020).
69. P. S. Chowdhury, K. Chamoto, A. Kumar, T. Honjo, PPAR-induced fatty acid oxidation in T cells increases the number of tumor-reactive CD8<sup>+</sup> T cells and facilitates anti-PD-1 therapy. *Cancer Immunol. Res.* **6**, 1375–1387 (2018).
70. M. D. Brand, D. G. Nicholls, Assessing mitochondrial dysfunction in cells. *Biochem. J.* **435**, 297–312 (2011).